Reactivating endogenous mechanisms of cardiac regeneration via paracrine boosting using the human amniotic fluid stem cell secretome

Carolina Balbi [a,b], Kirsten Lodder [c], Ambra Costa [a], Silvia Moimas [d], Francesco Moccia [e], Tessa van Herwaarden [c], Vittorio Rosti [f], Francesca Campagnoli [a], Agnese Palmeri [g], Pierangela De Biasio [g], Francesco Santini [h], Mauro Giacca [d], Marie-José Goumans [c], Lucio Barile [b], Anke M. Smits [c,1], Sveva Bollini [a,*,1]

[a] Regenerative Medicine Laboratory, Department of Experimental Medicine, University of Genova, Genova, Italy
[b] Molecular and Cell Cardiology Laboratory, CardioCentro Ticino, Lugano, Switzerland
[c] Department of Cell and Chemical Biology, Leiden University Medical Center, Leiden, the Netherlands
[d] Molecular Medicine Laboratory, International Centre for Genetic Engineering and Biotechnology (ICGEB), Trieste, Italy
[e] General Physiology Laboratory, Department of Biology and Biotechnology "Lazzaro Spallanzani", University of Pavia, Pavia, Italy
[f] Laboratory of Biochemistry, Biotechnology and Advanced Diagnostic, Myelofibrosis Study Centre, IRCCS Ospedale Policlinico San Matteo, Pavia, Italy
[g] Dept. of Obstetrics and Gynecology, IRCCS Ospedale Policlinico San Martino, Genova, Italy
[h] Division of Cardiac Surgery, IRCCS Ospedale Policlinico San Martino, Genova, Italy

ARTICLE INFO

Article history:
Received 30 May 2018
Received in revised form 29 March 2019
Accepted 3 April 2019
Available online 4 April 2019

ABSTRACT

Background: The adult mammalian heart retains residual regenerative capability via endogenous cardiac progenitor cell (CPC) activation and cardiomyocyte proliferation. We previously reported the paracrine cardioprotective capacity of human amniotic fluid-derived stem cells (hAFS) following ischemia or cardiotoxicity. Here we analyse the potential of hAFS secretome fractions for cardiac regeneration and future clinical translation.
Methods: hAFS were isolated from amniotic fluid leftover samples from prenatal screening. hAFS conditioned medium (hAFS-CM) was obtained following hypoxic preconditioning. Anti-apoptotic, angiogenic and proliferative effects were evaluated on rodent neonatal cardiomyocytes (r/mNVCM), human endothelial colony forming cells (hECFC) and human CPC. Mice undergoing myocardial infarction (MI) were treated with hAFS-CM, hAFS-extracellular vesicles (hAFS-EV), or EV-depleted hAFS-CM (hAFS-DM) by single intra-myocardial administration and evaluated in the short and long term.
Results: hAFS-CM improved mNVCM survival under oxidative and hypoxic damage, induced Ca^{2+}-dependent angiogenesis in hECFC and triggered hCPC and rNVCM proliferation. hAFS-CM treatment after MI counteracted scarring, supported cardiac function, angiogenesis and cardiomyocyte cell cycle progression in the long term. hAFS-DM had no effect. hAFS-CM and hAFS-EV equally induced epicardium WT1+ CPC reactivation. Although no CPC cardiovascular differentiation was observed, our data suggests contribution to local angiogenesis by paracrine modulation. hAFS-EV alone were able to recapitulate all the beneficial effects exerted by hAFS-CM, except for stimulation of vessel formation.
Conclusions: hAFS-CM and hAFS-EV can improve cardiac repair and trigger cardiac regeneration via paracrine modulation of endogenous mechanisms. While both formulations are effective in sustaining myocardial renewal, hAFS-CM retains higher pro-angiogenic potential, while hAFS-EV particularly enhances cardiac function.

1. Introduction

Heart failure (HF) affects 38 million people worldwide [1]. A major contributor to HF is myocardial infarction (MI) in which the reparative response results in collagen-enriched scarring induced by activated myofibroblasts [2,3]. Although this healing response prevents cardiac rupture, maladaptive remodelling disrupts cardiac function, resulting in HF.

Restoration of the injured heart requires (i) efficient cardioprotection, (ii) sustained neovascularisation, and (iii) myocardial renewal. Enduring cardiomyocyte survival during injury is critical for preservation of viable myocardium, while modulation of early inflammation and promotion of local angiogenesis improve repair process and counteract pathological remodelling.

Recent studies highlighted that the adult mammalian heart harbours an endogenous restorative programme mediated by resident cardiac progenitor cells (CPC) likely through paracrine contribution. CPC can

* Corresponding author at: Department of Experimental Medicine (DIMES) - University of Genova, Genova, Italy.
E-mail address: sveva.bollini@unige.it (S. Bollini).
[1] These authors contributed equally to the study.

improve cardiomyocyte survival, angiogenesis and cardiac function following MI [4]. Several CPC have been described, with growing interest in the epicardium-derived progenitor cells from which part of coronary vasculature and, possibly, ventricular cardiomyocytes are derived during heart development [5]. These cells provide regenerative potential in the injured adult heart, particularly after priming by paracrine signals [6,7]. Furthermore, the long-held dogma that terminally differentiated mammalian cardiomyocytes permanently exit cell cycle has been dismissed. Although mitotic cardiomyocytes precipitously decrease during life, a renewal rate of 0.5–1% per year has been reported in humans [8,9]. Interestingly, CPC activation and myocardial renewal are highly responsive in the damaged neonatal heart, yet this reparative potential is lost by seven days of age [10,11]. Reactivation of these response mechanisms in the adult myocardium would be a major therapeutic breakthrough to reduce loss of cardiac function after injury.

Most stem cells transplanted in the injured heart were shown to act via paracrine mechanisms enhancing survival and function of endogenous cells [12]. Thus, increasing attention has been given to the stem cell *secretome* as working therapeutic strategy. Human amniotic fluid stem cells (hAFS) are broadly multipotent mesenchymal progenitors isolated from leftover samples of amniotic fluid, via prenatal amniocentesis screening [13] or during scheduled C-section procedure [14]. We previously demonstrated that the hAFS secretome prompt cardioprotective paracrine potential in a preclinical rat model of myocardial ischemia/reperfusion injury [15]. Additionally, hAFS medium conditioned under hypoxia, exerted remarkable pro-survival effects on murine cardiomyocytes and on human CPC in a doxorubicin-induced cardiotoxicity model, by modulating their response to injury [16].

Here we report further investigation on hAFS secretome-derived cardioprotection, long term cardiac repair and activation of endogenous regenerative programme via stimulation of epicardial cell activity and induction of cardiomyocyte cell cycle progression.

2. Methods

An extended version is reported in the Supplementary Methods and in the Data in Brief article, here indicated as reference [17].

2.1. Cell culture

hAFS were obtained from left over amniotic fluid sample from prenatal amniocentesis screening [16,18]. Human NCTC 2544 keratinocytes were purchased (Interlab Cell Line Collection, Genova, Italy). Human circulating endothelial colony-forming cells (hECFC) and human adult CPC were obtained as described in [17]. Human adult epicardium derived progenitor cells (hEPDC) were isolated as in [19,20]; the epicardial tissue was digested by three rounds of incubation in a 0.25% Trypsin/EDTA solution (Serva, Heidelberg, Germany). Cells were cultured on 0.1% gelatin coated dishes in Dulbecco's modified Eagle's medium (DMEM-glucose low; Invitrogen, Carlsbad, California) and Medium 199 (M199; Invitrogen, Carlsbad, California) supplemented with 10% heat-inactivated FCS (Gibco-Thermo Fisher Scientific, Waltham, Massachusetts), and 100 U/ml penicillin/streptomycin (Gibco-Thermo Fisher Scientific, Waltham, Massachusetts).

Mouse and rat neonatal ventricular cardiomyocytes (m/rNVCM) were obtained as in [17]. Human cell isolation was performed following informed consent and conformed to the 1975 Declaration of Helsinki and specific authorization (P.R. 428REG2015; P.R.007REG2013; P08.087 and n.20110004143).

2.2. Collection of cell-conditioned medium and EV isolation

Cell-conditioned medium (hAFS-CM and hNCTC-CM) was isolated following hypoxic preconditioning of cells [16]. hAFS-extracellular vesicles (hAFS-EV) were produced by serial ultracentrifugation [18]. hAFS-CM depleted of hAFS-EV (hAFS-DM) was obtained as remaining solution after hAFS-EV isolation.

2.3. Cytokine profiling of cell secretome

Cell secretome cytokine and chemokine profiling was performed by Proteome Profiler™ Human XL Cytokine Array kit (R&D System, Minnesota, US) as in [17].

2.4. In vitro analysis of hAFS secretome paracrine potential

Anti-apoptotic, pro-angiogenic and proliferative effects were tested on m/rNCVM, hECFC and hCPC as in [17].

2.5. In vivo analysis of hAFS secretome paracrine potential

C57BL/6 (n = 60) and $Wt1^{CreERT2/+}$;$R26R^{mTmG/+}$ mice (n = 60) labelling EPDC by embryonic gene Wt1 expression [21] were used, according to the Italian Ministry of Health (n.384/2016-PR) and the Committee on Animal Welfare of Leiden University Medical Center (PE.13353001) authorizations (EU Directive 2010/63/EU). MI injury was induced as previously described [7]. 100 μg of hAFS-CM or hAFS-DM or 4.5 μg of hAFS-EV versus vehicle serum-free medium (Ctrl) were injected in the peri-infarct area. Echocardiography was performed at 7 and 28 days after MI on a Vevo 770 High-Resolution In Vivo Micro-Imaging System (VisualSonic, Toronto, Canada). Left ventricular ejection fraction (%LVEF) was calculated from left ventricle-tracing on long axis ECG-gated Kilohertz Visualization (EKV) recordings. Hearts were harvested at 3 h, 24 h, 7- and 28 days following MI for histological evaluation. Images were acquired on a Pannoramic Slide Scanner (3dhistech, Budapest, Hungary). Confocal images were acquired on a Leica SP5 confocal microscopy (Leica, Wetzlar, Germany).

2.6. Statistical analysis

Results are presented as mean ± s.e.m. (standard error of mean) of at least three (n = 3) independent replicated experiments. Comparisons were drawn by one-way ANOVA followed by post-hoc Tukey's multiple test or by unpaired *t*-test (when appropriate) and analysed by Prism Version 6.0a GraphPad Software with statistical significance defined as $^{*}p < 0.05$.

3. Results

3.1. The human AFS secretome mediates pro-survival, angiogenic and stimulatory effects in vitro

Since hAFS are activated by the ischemic environment [15], hypoxic preconditioning was adopted to supplement hAFS-CM with trophic factors. Hypoxic hAFS-CM showed a trend in enrichment of Macrophage Migration Inhibitor Factor (MIF), Interleukin 8 and 6 (IL-8, IL-6), Osteopontin (OPN), Fibroblast Growth Factor-19 (FGF-19), Monocyte Chemoattractant Protein-1 (MCP-1) and Growth Differentiation Factor-15 (GDF-15) while Stromal Derived Factor-1alpha (SDF-1α) and Plasminogen Activator Inhibitor-1 (PAI-1) were comparable to control. Hypoxic hAFS-CM was also supplemented with extracellular matrix metalloproteinase inducer (EMMPRIN) and insulin like growth factor binding protein 2 (IGFBP-2, Fig. 1, Table 1 in [17]).

Pre-treatment of mNVCM with hAFS-CM remarkably enhanced their survival under oxidative and hypoxic damage (Figure 2A–B in [17]). hAFS-CM-primed hECFC formed capillary-like networks, while hNCTC-CM did not trigger tube formation (Figure 2C in [17]). Length of endothelial tube-like structures (TLS), meshes and master junctions that developed by hAFS-CM instruction were significantly higher compared to basal medium and hNCTC-CM. Repetitive oscillations in intracellular Ca^{2+} concentration ($[Ca^{2+}]_i$) drive proliferation and tube formation in hECFC [22,23]. hAFS-CM caused robust intracellular Ca^{2+} oscillations in majority of hECFC, while hNCTC-CM triggered a biphasic increase not influencing either proliferation or tube formation (Figure 2D in [17]). Preventing $[Ca^{2+}]_i$ oscillations with 30 μM BAPTA, a membrane permeable intracellular Ca^{2+} buffer [22,23], inhibited tubulogenesis in hECFC challenged with hAFS-CM (Figure 2C in [17]). While hNCTC-CM didn't exert any influence, hAFS-CM significantly supported cell cycle progression by BrdU incorporation and Ki67 expression in adult hCPC, fetal Sca-1^{+} CPC, hEPDCc and hEPDCs (Fig. 3A–D, Figure 4 in [17]). This enhanced DNA replication was also observed in rNVCM as their EdU incorporation significantly increased (Figure 3E in [17]). In contrast, the hNCTC secretome displayed a limited effect compared to the hAFS secretome. These results were further confirmed on less responsive rNVCM from 5-day-old rat hearts (Figure 3F in [17]). EdU-positive rNCVM percentage notably increased upon hAFS-CM treatment over untreated cells (Ctrl), while hNCTC-CM did not significantly affect cardiomyocyte behaviour.

3.2. The hAFS secretome enhances myocardial repair following MI

When animals undergoing MI received intramyocardial injections of hAFS-CM, a significant decrease in cell apoptosis was observed 24 h

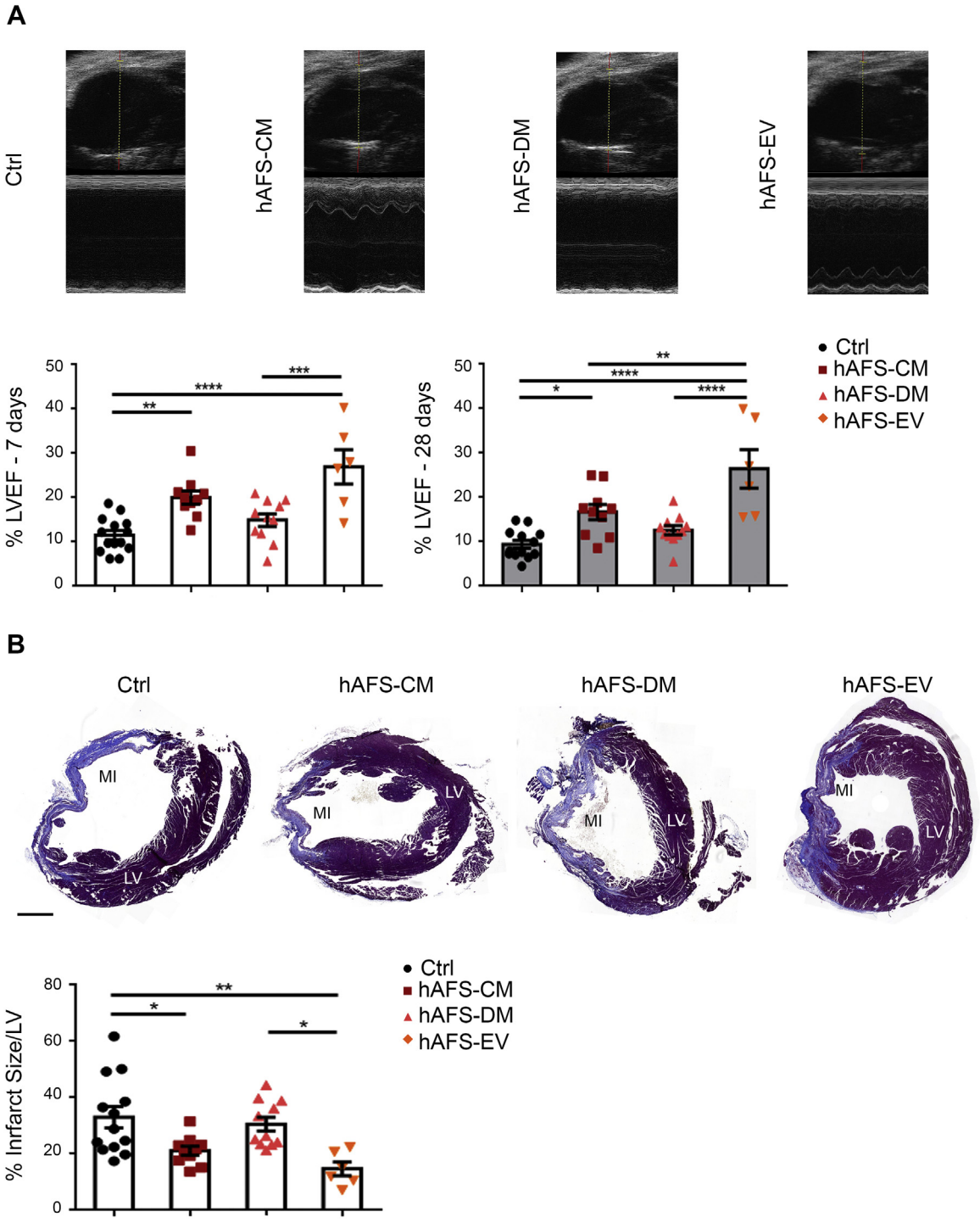

Fig. 1. hAFS secretome enhances cardiac repair following MI. A) Evaluation of cardiac function by percentage of left ventricular ejection fraction (%LVEF) in mice assessed at 7 and 28 days post MI and treated with 100 μg hAFS-CM or hAFS-DM or 4.5 μg hAFS-EV over serum-free vehicle solution (Ctrl) by intra-myocardial injection (7 days post-MI: Ctrl: 11.53 ± 1.04%, n = 14; hAFS-CM: 20.03 ± 1.50%, n = 10; hAFS-DM: 14.92 ± 1.42%, n = 11; hAFS-EV: 26.96 ± 3.85%, n = 6; $^{***}p < 0.001$, $p = 0.0001$; $^{***}p < 0.001$, $p = 0.0005$ and $^{**}p < 0.01$, $p = 0.0026$; 28 days post-MI: Ctrl: 9.40 ± 0.90%, n = 13; hAFS-CM: 16.70 ± 1.72%, n = 10; hAFS-DM: 12.62 ± 1.01%, n = 11; hAFS-EV: 26.44 ± 4.33%, n = 6; $^{****}p < 0.0001$; $^{**}p < 0.01$, $p = 0.007$ and $^{*}p < 0.05$, $p = 0.015$). Upper panel: representative ultrasound images at 28 days. B) Pathological remodelling at 28 days post-MI in mice treated with 100 μg hAFS-CM or hAFS-DM or 4.5 μg hAFS-EV over serum-free vehicle solution (Ctrl) by intra-myocardial injection. The infarct size was evaluated by Masson's Trichrome staining as percentage of the collagen scar area over total left ventricle area (Ctrl: 33.04 ± 3.80%, n = 13; hAFS-CM: 21.12 ± 1.62%, n = 10; hAFS-DM: 30.60 ± 2.50%, n = 11; hAFS-EV: 14.70 ± 2.44%, n = 6; $^{**}p < 0.01$, $p = 0.0024$, $^{*}p < 0.05$, $p = 0.027$ and $p = 0.012$). Upper panel: representative pictures of histological analyses, scale bar 1000 μm. *MI: myocardial infarct; LV: left ventricle.*

after MI compared to vehicle-treatment (Supplementary Fig. 1A). hAFS-CM curbed down the acute inflammatory response, since infiltrating MPO-positive neutrophils and CD68-positive macrophages were considerably reduced (Supplementary Fig. 1B–C). Modulation of inflammation was confirmed by a remarkable decrease in *Il1α* and *Mpo* expression (Supplementary Fig. 1D). We then moved onwards by (i) analysing the long-term effects after a single secretome administration in the acute setting and (ii) dissecting which component may be relevant in driving beneficial responses. Both the total cell-conditioned medium (hAFS-CM) and the extracellular vesicles (hAFS-EV) were able to sustain cardiac function shown by a significantly higher %LVEF, compared to Ctrl at 7 days post-MI (1.7- and 2.3-fold, respectively).This positive response

was maintained up to 28 days, with hAFS-CM and hAFS-EV resulting in a 1.8 and 2.8-fold higher LVEF compared to Ctrl, respectively (Fig. 1A); hAFS-EV showed a 1.5-fold superior influence compared to hAFS-CM in the long-term. Importantly, hAFS-medium depleted of EV (hAFS-DM) did not exert any effect. Within the hAFS-CM and Ctrl group we did not detect any significant variation in %LVEF values over time.

Single acute administration of hAFS-CM or hAFS-EV influenced pathological remodelling at 28 days post-MI, with a reduced infarct size (by 36% and 56% over control mice, respectively). On the contrary, hAFS-DM resulted in a comparable infarct area by collagen scar to control animals (Fig. 1B).

28 days post-MI local angiogenesis was considerably increased by hAFS-CM treatment only (Fig. 2A). Micro-vessel density by PECAM-1-positive expression was significantly raised by 1.8-fold within the injured myocardium compared to the control group. Similarly, αSMA-positive vessels were increased. When applying Feret diameter measurement

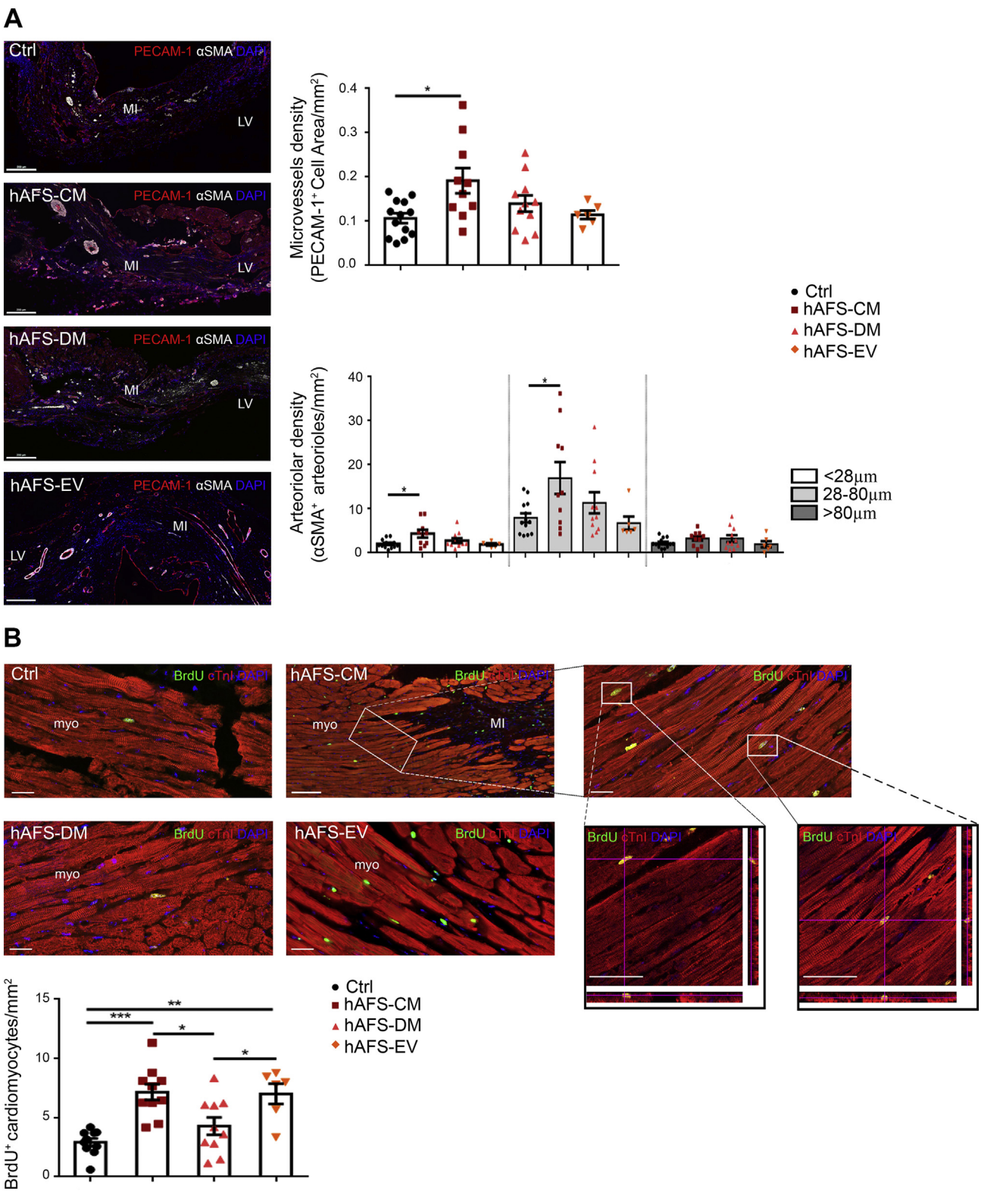

[24], we only noticed a significant increase in very small- (<28 μm) and medium-sized (28–80 μm) arterioles with hAFS-CM stimulation (2.1-fold over control). Both hAFS-EV and hAFS-DM did not influence new vessel development.

hAFS-CM activated cell-cycle re-entry of adult resident cardiomyocytes, as revealed by BrdU and cTnI staining at 28 days post-MI (Fig. 2B). BrdU-positive cardiomyocytes were found in the peri-infarct zone as significantly increased by 2.5-fold when primed with hAFS-CM, compared to vehicle-treated mice, and by 1.7-fold related to hAFS-DM, which did not induce any relevant effect. hAFS-EV exerted a stimulatory effect similarly to hAFS-CM, as supported by the increase of BrdU incorporation by resident cardiomyocytes by 2.4- and 1.6-fold over Ctrl and hAFS-DM treated mice, respectively.

3.3. The hAFS secretome triggers the cardiac endogenous regenerative programme

Since in vitro data suggested that hAFS-CM is able to induce CPC activation, we pursued this effect in vivo, by employing a tamoxifen inducible $Wt1^{CreERT2/+}$;$R26R^{mTmG/+}$ mouse line to pulse label WT1+ EPDC via GFP expression [21]. hAFS-CM injection boosted the activation of adult WT1+ EPDC by 2.7-fold, compared to control mice and by 2.4-fold over hAFS-DM, which didn't contribute significantly (Fig. 3A). Similarly, hAFS-EV recapitulated the whole secretome (hAFS-CM) effect, as increasing WT1+ EPDC by 2.5- and 2.2-fold related to control and hAFS-DM treated mice, respectively, with no difference over hAFS-CM (Fig. 3A). Histological analysis at 7 and 28 days after MI indicated that GFP+ EPDC did not migrate away from the epicardium nor matured into PECAM-1, αSMA, or cTnI-positive cells and their levels decreased at 28 days after MI (Fig. 3B, Supplementary Fig. 2).

GFP-negative and BrdU-positive cardiomyocytes were found starting at 7 days post-MI in $Wt1^{CreERT2/+}$;$R26R^{mTmG/+}$ mice treated with control vehicle solution, and almost tripled following either hAFS-CM or hAFS-EV stimulation. hAFS-CM was more effective than hAFS-DM, which did not contribute significantly (Fig. 3C). Since hAFS-EV are loaded with microRNAs (miRNA) [18] involved in cell cycle re-entry of adult mature cardiomyocyte [25–27], we evaluated whether resident adult cardiomyocytes cell cycle re-entry was mediated horizontal transfer of miRNA to the myocardial tissue by hAFS-EV. Three hours after MI and hAFS-EV administration, we detected a positive trend of up-regulation of the cardio-active miR-210, miR-199a-3p, and a more specific enhancement of miR-146a (Supplementary Fig. 3).

3.4. The hAFS secretome could trigger a paracrine cascade on resident cardiac cells

EPDC activation was increased in hAFS-CM treated animals; these cells are known to influence their surroundings via paracrine effects [6,28]. As well, hAFS-CM showed to be the secretome formulation supporting local angiogenesis. Thus, we primed in vitro cultured adult human EPDC with hAFS-CM and employed the resulting hEPDC-CM^{primed} in a Matrigel angiogenesis assay on HUVEC (Fig. 4A). Control hEPDC-CM was not effective in sustaining HUVEC tubulogenesis, compared to cells grown in angiogenic medium (positive control). hEPDC-CM^{primed} increased capillary-like TLS, junctions and number of branches, similarly to positive control. Priming by hAFS-CM resulted in a positive trend in the enrichment of PAI-1, IL-8, IGFBP-2, IL-4, IL-22, OPN, EMMPRIN, and to a lesser extent of SDF-1α, angiopoietin-2 (ANGPT-2), MCP-1 and FGF-19 in hEPDC-CM^{primed} versus control hEPDC-CM (Fig. 4B, Supplementary Table 1).

4. Discussion

The hAFS secretome has paracrine therapeutic cardio-active effects in a preclinical mouse model of MI. We showed that the hAFS secretome enhances cardiac repair and rescues long-term cardiac function by single administration soon after injury. It also stimulated re-activation of endogenous WT1+ EPDC and promoted cell cycle progression in resident cardiomyocytes, thereby supporting cardiac regeneration.

hAFS were preconditioned under hypoxia [16], with hAFS-CM enrichment of factors like IL-6, OPN, MIF and GDF-15. GDF-15 exerts pro-survival and anti-inflammatory effects and inhibits cardiac pathological remodelling following injury [29,30]. OPN-null mice undergoing MI increased heart dilation, underlining this factor relevance on cardiac microenvironment [31]; MIF is involved in preservation of cardiac homeostasis during physiological ageing, [32] while IL-6 modulates paracrine control of neonatal cardiomyocyte proliferation following injury [33,34].

Hypoxic hAFS-CM increased survival of neonatal mouse cardiomyocytes under oxidative or hypoxic injury. Such cardioprotective effect was further substantiated by suppression of myocardial inflammation and increased preservation of adult cardiomyocytes over the first 24 h post-MI, confirming previous findings [15]. Acute secretome administration had beneficial long-term consequences, with reduced infarct size and improved cardiac function a month after injury. Likewise, restoration of myocardial perfusion via neo-angiogenesis is essential for cardiac repair; hAFS have demonstrated remarkable angiogenic potential in various preclinical rodent models of tissue ischemia [14,35,36]. Here, hAFS-CM stimulated hECFC to activate intracellular Ca^{2+} oscillations, which selectively triggered proliferation and tubulogenesis in the treated cells [22,37–39]. We also observed significant intensification of neovascularization following intra-myocardial injection of hAFS-CM, with increased number of arteriole-like vessels in the injured myocardium.

Cardiomyocyte reconstitution is pivotal for cardiac regeneration [4,40]. We demonstrate that hAFS secretome stimulates cell cycle progression in cultured rodent neonatal cardiomyocytes. Importantly, the number of BrdU-incorporating adult cardiomyocytes was significantly increased after hAFS injection in vivo, indicative of increased myocardial regenerative potential.

Interestingly, administration of the secretome soluble fraction after depletion of the EV content (hAFS-DM) failed to elicit the hAFS paracrine beneficial effects, suggesting their key role in orchestrating

Fig. 2. hAFS secretome sustains local angiogenesis and cardiomyocyte cell cycle progression following MI. A) Analysis of local angiogenesis via assessment of micro-vessel density by PECAM-1-positive and αSMA-positive arterioles in the infarct border area at 28 days post MI in mice treated with 100 μg hAFS-CM or hAFS-DM 4.5 μg hAFS-EV over serum-free vehicle solution (Ctrl) by intra-myocardial injection. Right upper panel: PECAM-1 positive expression; Ctrl: 0.11 ± 0.01 $PECAM\text{-}1^+$ Cell Area/mm^2, n = 13; hAFS-CM: 0.19 ± 0.03 $PECAM\text{-}1^+$ Cell Area/mm^2, n = 10; hAFS-DM: 0.14 ± 0.02 $PECAM\text{-}1^+$ Cell Area/mm^2, n = 11; hAFS-EV: 0.12 ± 0.01 $PECAM\text{-}1^+$ Cell Area/mm^2, n = 6; $^*p < 0.05$, $p = 0.011$. Right lower panel: αSMA-positive arterioles as divided by vessel diameter into small (<28 μm), medium (28–80 μm) and big (>80 μm) size. Small-size arterioles: Ctrl: 2.03 ± 0.30 αSMA^+ arterioles/mm^2, n = 13; hAFS-CM: 4.40 ± 0.90 αSMA^+ arterioles/mm^2, n = 10; hAFS-DM: 2.80 ± 0.53 αSMA^+ arterioles/mm^2, n = 11; hAFS-EV: 1.91 ± 0.24 αSMA^+ arterioles/mm^2, n = 6; $^*p < 0.05$, $p = 0.018$. Medium-size arterioles: Ctrl: 7.94 ± 1.01 αSMA^+ arterioles/mm^2, n = 13; hAFS-CM: 17.00 ± 3.62 αSMA^+ arterioles/mm^2, n = 10; hAFS-DM: 11.40 ± 2.40 αSMA^+ arterioles/mm^2, n = 11; hAFS-EV: 6.75 ± 1.50 αSMA^+ arterioles/mm^2, n = 6; $^*p < 0.05$, $p = 0.03$. Big-size arterioles: Ctrl: 2.21 ± 0.30 αSMA^+ arterioles/mm^2, n = 13; hAFS-CM: 3.25 ± 0.51 αSMA^+ arterioles/mm^2, n = 10; hAFS-DM: 3.25 ± 0.80 αSMA^+ arterioles/mm^2, n = 11; 1.99 ± 0.71 αSMA^+ arterioles/mm^2, n = 6. Left panel: representative images of cardiac tissue stained for PECAM-1 (red); αSMA (white) and DAPI (blue) in the infarct border area; scale bar: 50 μm. B) Assessment of cardiomyocyte cell cycle progression by BrdU incorporation via co-expression with cTnI at 28 days post-MI in mice treated with 100 μg hAFS-CM or hAFS-DM or 4.5 μg hAFS-EV over vehicle solution (Ctrl) by intra-myocardial injection (Ctrl: 2.91 ± 0.33 $BrdU^+$ cardiomyocytes/mm^2, n = 10; hAFS-CM: 7.20 ± 0.70 $BrdU^+$ cardiomyocytes/mm^2, n = 10; hAFS-DM: 4.30 ± 0.74 $BrdU^+$ cardiomyocytes/mm^2, n = 10; hAFS-EV: 7.01 ± 0.86 $BrdU^+$ cardiomyocytes/mm^2, n = 6; $^{***}p < 0.001$, $p = 0.0002$; $^{**}p < 0.01$, $p = 0.0015$; $^*p < 0.05$, $p = 0.011$ and $p = 0.048$). Upper panel: representative images of myocardial tissue stained for cTnI (red); BrdU (green) and DAPI (blue) in the infarct border area; scale bar: 50 μm and 100 μm. Inlet magnifications showing confocal microscopy analysis of BrdU+ nuclei. *MI: myocardial infarct; LV: left ventricle; PECAM-1: Platelet and Endothelial Cell Adhesion Molecule-1; αSMA: alpha Smooth Muscle Actin.*

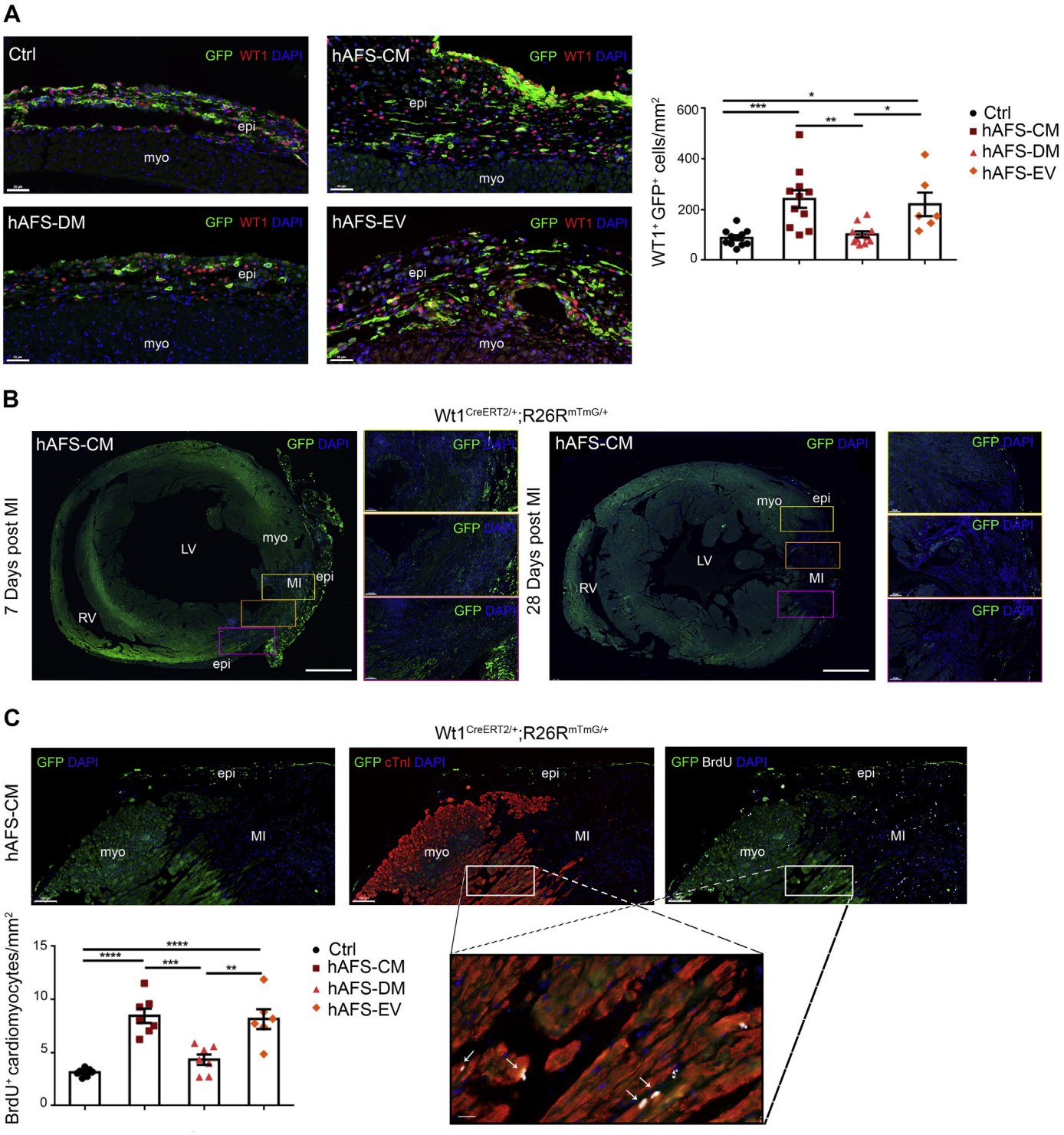

Fig. 3. *hAFS secretome triggers endogenous regenerative mechanisms.* A) Re-activated WT1^{+} EPDC traced by GFP labelling in Wt1$^{CreERT2/+}$;R26R$^{mTmG/+}$ mice at 7 days post-MI and following intra myocardial injection of either 100 μg hAFS-CM, hAFS-DM or 4.5 μg hAFS-EV, versus serum-free vehicle-treated (Ctrl) animals (Ctrl: 88.30 ± 9.72 WT1^{+} GFP^{+} cells/mm^2, n = 11; hAFS-CM: 241.50 ± 34.93 WT1^{+} GFP^{+} cells/mm^2, n = 11; hAFS-DM: 101.40 ± 11.60 WT1^{+} GFP^{+} cells/mm^2, n = 11; hAFS-EV: 220.80 ± 46.64 WT1^{+} GFP^{+} cells/mm^2, n = 6, ***p < 0.001, p = 0.0004; *p < 0.05, p = 0.0127 and p = 0.0285; **p < 0.01, p = 0.0013). Left panel: representative images of heart tissue at 7 days post-MI stained for WT1 (red); GFP (green) and DAPI (blue), scale bar: 50 μm. B) Representative pictures of Wt1$^{CreERT2/+}$R26R$^{mTmG/+}$ mouse heart sections showing WT1^{+} EPDC reactivation as assessed by GFP staining (green) within 7 days post MI and their decrease at 28 days following injury; scale bar: 1000 μm and 100 μm in inlet magnifications. C) Representative images of cardiac tissue from Wt1$^{CreERT2/+}$;R26R$^{mTmG/+}$ mice treated with hAFS-CM at 7 days post-MI, showing no expression of GFP (green) in cTnI-(red) and BrDU-positive (white nuclei) cardiomyocytes in the infarct border area; scale bar: 100 μm and 20 μm in the inlet magnification. Evaluation of GFP-negative BrDU-positive resident cardiomyocytes at 7 days post-MI and following intra-myocardial injection of either 100 μg hAFS-CM or hAFS-DM or 4.5 μg hAFS-EV versus Ctrl animals (Ctrl: 3.13 ± 0.14 BrdU^{+} cardiomyocytes/mm^2, n = 11; hAFS-CM: 8.50 ± 0.70 BrdU^{+} cardiomyocytes/mm^2, n = 11; hAFS-DM: 4.34 ± 0.50 BrdU^{+} cardiomyocytes/mm^2, n = 11; hAFS-EV: 8.15 ± 0.93 BrdU^{+} cardiomyocytes/mm^2, n = 6; *****p < 0.0001, ***p < 0.001, p = 0.0003, **p < 0.01, p = 0.001). *Epi: epicardium; Myo: myocardium; MI: myocardial infarct.*

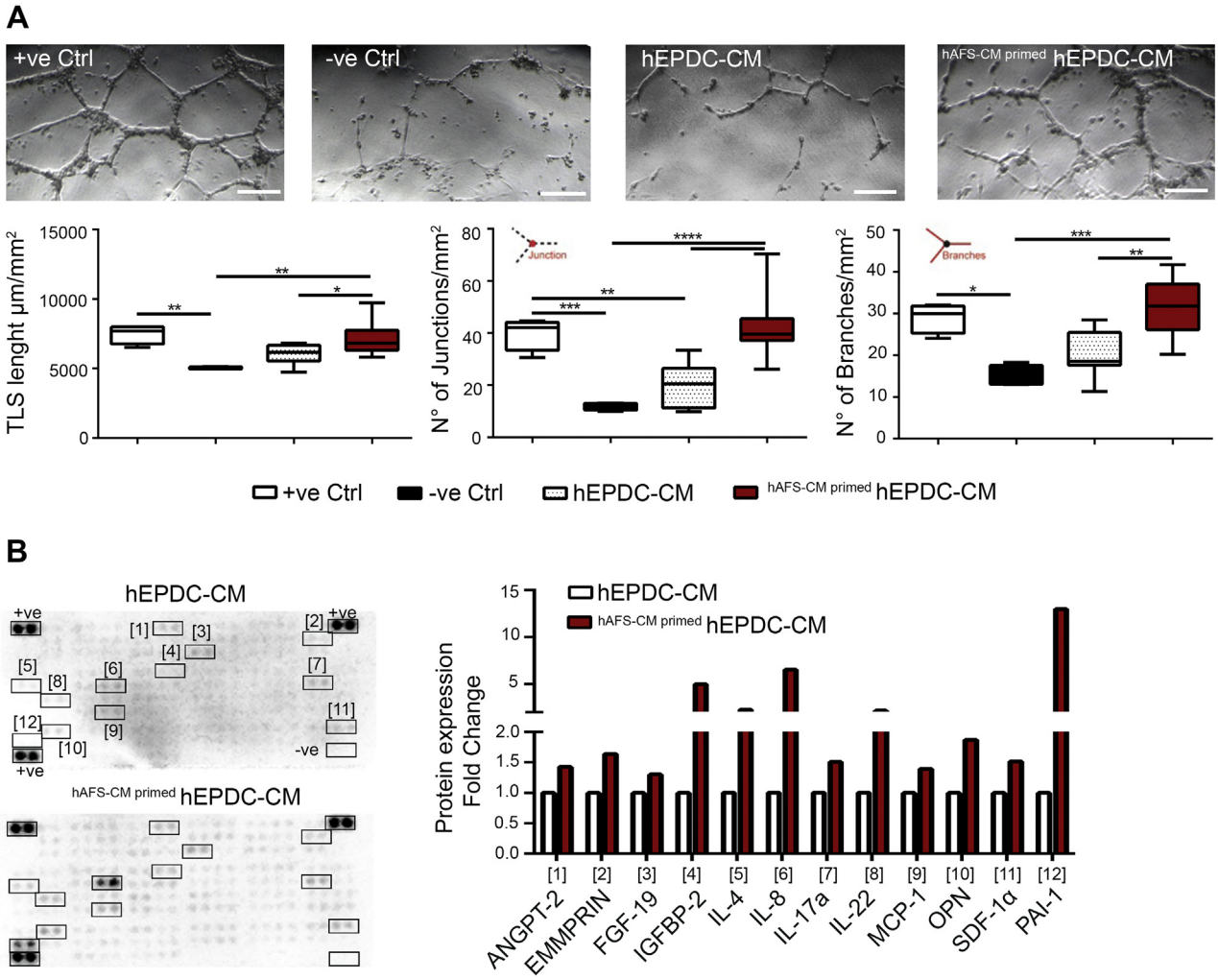

Fig. 4. Paracrine cascade of action. A) In vitro HUVEC tubulogenesis following incubation with: untreated control hEPDC-CM or hEPDC-CM^{primed}, compared to cells grown in EGM-2 endothelial medium as positive control (+ve Ctrl) or to cells grown in 1% FBS hEPDC basal medium (−ve Ctrl). Representative images were obtained 18 h after plating cells in Matrigel; scale bar: 50 µm. Lower panel, evaluation of TLS, junction and branches developed by HUVEC. (TLS total length, n = 4 experiments; +ve Ctrl: 7489 ± 341.4 µm/mm^2, −ve Ctrl: 5044 ± 39.34 µm/mm^2, hEPDC-CM: 6011 ± 266.1 µm/mm^2, hEPDC-CM^{primed}: 7147 ± 282.3 µm/mm^2, $^*p < 0.05$, $p = 0.0436$, $^{**}p < 0.01$, $p = 0.0028$ and $p = 0.0013$); number of junctions, n = 4 experiments, +ve Ctrl: 39.81 ± 3.14 junctions/mm^2, −ve Ctrl: 11.89 ± 0.70 junctions/mm^2, hEPDC-CM: 19.32 ± 3.26 junctions/mm^2, hEPDC-CM^{primed}: 41.96 ± 2.72 junctions/mm^2, $^{**}p < 0.01$, $p = 0.005$, $^{***}p < 0.001$, $p = 0.0007$, $^{****}p < 0.0001$; number of branches, n = 4 experiments, +ve Ctrl: 28.99 ± 1.77 branches/mm^2; −ve Ctrl: 14.99 ± 1.22 branches/mm^2, hEPDC-CM: 20.36 ± 2.16 branches/mm^2; hEPDC-CM^{primed}: 31.24 ± 1.79 branches/mm^2; $^*p < 0.05$, $p = 0.0109$, $^{**}p < 0.01$, $p = 0.0022$, and $^{**}p < 0.001$, $p = 0.0002$. B) Cytokine and chemokine array of hEPDC-CM^{primed} versus control hEPDC-CM by quantification of positive pixels for each cytokine. Left panel: representative images of array membranes in which numbers indicate the corresponding chemokine/cytokine in the graph below. Values are expressed as fold change over hEPDC-CM and reported in Supplementary Table 1. *HUVEC: Human Umbilical Vein Endothelial Cells; +ve Ctrl: positive control; +ve: positive reference control; −ve: negative reference control.*

reparative responses. We recently described hAFS-EV as biological conveyors of proliferative, anti-inflammatory and anti-apoptotic effects, with a putative mechanism of action involving horizontal transfer of miRNAs into responder cells [18]. In this study, we found that hAFS-EV could recapitulate most of hAFS-CM long-term effects in vivo, when directly compared to the total secretome and to the remaining soluble fraction. hAFS-EV remarkably improved cardiac function and reduced collagen deposition and pathological remodelling; indeed, the immunomodulatory potential of hAFS-EV may explain the reduction in the infarct size, as recently confirmed in a subsequent independent study [41]. Notably, isolated EV seemed even more effective than hAFS-CM in supporting LVEF at 4 weeks after MI. On the contrary, they were unable to provoke any significant pro-angiogenic effects. This is in accordance with our previous findings showing that in vivo angiogenic potential of hAFS-EV may be dose-dependent [18]. hAFS-EV primarily contain miRNAs with pro-survival, immunomodulatory and proliferative effects [18]. Thus, in order to exert significant pro-angiogenic influence, they might synergistically combine their paracrine actions with the soluble counterpart of hAFS-DM. Yet, a single injection of hAFS-EV alone promoted resident surviving cardiomyocyte cell cycle progression 4 weeks after injury to the same extent as hAFS-CM; both hAFS-EV and hAFS-CM showed a superior cardiomyogenic renewal potential over the hAFS-DM soluble counterpart. This was confirmed by the enrichment of regenerative miRNA detected within the mouse myocardial tissue 3 h following hAFS-EV administration; we found significantly increased expression of miR-146a, which is well-known to promote cardiomyocyte proliferation via CPC-exosomes [27] and to be present in hypoxic hAFS-EV [18]. Likewise, a positive trend in the enrichment for the hAFS-EV-specific cardio-active and proliferative miR-210 [26] and miR-199a-3p [25] was detected.

We also investigated whether long-term therapeutic effects of the hAFS secretome were due to early activation of resident CPC. Our in vitro data showed a remarkable proliferative influence of the hAFS secretome on several subpopulations of fetal and adult CPC, also including both resting and EMT-activated human EPDC. In vivo in the adult heart, epicardial cells become quiescent soon after birth, downregulating their embryonic plasticity, but maintaining partial responsive capacity following injury, with limited cardiomyogenic potential [7,42–44].

Within a week from injury and intra-myocardial administration of hAFS-CM or EV, we observed a dramatic increase in endogenous EPDC re-activating the key embryonic epicardial gene *Wt1*, associated with their expansion. Nonetheless, we observed that reactivated $WT1^+$ GFP^+ EPDC remained confined to the sub-epicardial layer, without signs of migration nor differentiation. Paracrine stimulation by hAFS-CM and hAFS-EV activates *Wt1* expression in resident EPDC, yet without contribution to de novo cardiac cells. Our results are in line with studies reporting that MI triggers proliferation of resident EPDC, without differentiation into cardiomyocytes or endothelial cells, but with paracrine effects on local myocardial neovessel network expansion [6,45]. It is therefore conceivable that hAFS secretome enhances $WT1^+$ EPDC reactivation by triggering a paracrine cascade mechanism and boosting the proliferative and secretory potential of epicardial CPC. Additional in vitro analyses supported this working hypothesis, since human EPDC primed by hAFS-CM developed an angiogenic secretome enriched of EMT-driven paracrine chemokines, endothelial activators and pro-angiogenic factors, such as EMMPRIN [46] IGFBP-2 [47], IL-4 and IL-8 [48], and PAI-1 [49] that significantly increase tubulogenesis by HUVEC cells.

In summary, we identified total hAFS-CM as the most efficient secretome formulation to promote cardiac tissue repair and to stimulate cardiac regeneration. Isolated hAFS-EV can recapitulate most of the cardio-active and myocardial regenerative effects obtained with hAFS-CM and showed a stronger effect in supporting cardiac function in the long term; yet, they might not represent an ideal therapeutic candidate to trigger local angiogenesis. Hence, according to specific therapeutic necessities (i.e. enhancement of neovascularization or rescue of cardiac function), hAFS-CM can be preferred over hAFS-EV.

4.1. Limitations of the study

Limitations of the present study must be acknowledged and need to be addressed with further research. Follow up administration of hAFS-CM or hAFS-EV has not been investigated; we cannot exclude that absence of $WT1^+$ EPDC cardiomyogenic and cardiovascular commitment might be explained by lack of sustained stimulation. Since detailed tracking of adult cardiomyocyte cell cycle re-entry is currently debated and controversial, detailed analysis is required to better assess cell cycle progression over functional cytokinesis. Moreover, additional investigation is required to evaluate paracrine effect of hAFS-EV on resident murine EPDC in potentiating angiogenesis and/or cell proliferation.

5. Conclusions

The hAFS secretome is endowed with remarkable paracrine potential to restore cardiac endogenous mechanisms otherwise forgotten, thus representing an appealing future *pharmacotherapeutic agent.* The ideal stem cell source for paracrine therapy should be selected upon secretory potential and isolation feasibility. Adult stem cells present several limitations: low yield, invasive sampling and controversial self-renewal, all of which limit their therapeutic applicability. On the contrary, fetal/perinatal stem cells, like hAFS, can be easily isolated from discarded samples via prenatal screening or as clinical waste after birth.

Supplementary data to this article can be found online at https://doi.org/10.1016/j.ijcard.2019.04.011.

Author contribution

C.B.: conception, collection, analysis and interpretation of data, manuscript writing, and final approval; K.L.: CPC culture, MI surgical model, ultrasound analysis, final approval; A.C.: cell secretome collection and processing; final approval; S.M.: rNVCM analysis; final approval; F.M.: Ca^{2+} analysis; manuscript writing and final approval; T.vH.: EPDC culture, collection of data, final approval; V.R.: hECFC analysis; final approval; F.C.: experiment assistance; final approval; A.P.: provision of human amniotic samples; final approval; P.D.B.: provision of human amniotic samples; final approval; F.S.: provision of human cardiac specimens; final approval; M.G. final approval; M.J.G.: data interpretation, final approval; L.B.: data interpretation, manuscript writing; final approval; A.S: conception and design; financial support; data interpretation; manuscript writing; final approval; S.B.: conception and design; MI surgical model; financial support; data interpretation; manuscript writing and final approval.

Grant support

This work has been funded by *Programma Giovani Ricercatori "Rita Levi Montalcini" (Bando 2012)* from the Italian Ministry of Education, University and Research (MIUR) to S. Bollini and by a Leiden University Medical Center (LUMC) and a Dekker Fellowship (senior scientist, 2017T059) from the Dutch Heart Foundation to A.M. Smits.

Declaration of interest

Authors report no relationships that could be construed as a conflict of interest.

Acknowledgements

S.B. was funded by *Programma Giovani Ricercatori "Rita Levi Montalcini"* from the Italian Ministry of Education, University and Research; A.M.S. was supported by a Leiden University Medical Center (LUMC) research fellowship and a Dekker Fellowship (senior scientist, 2017T059) from Dutch Heart Foundation. This study contributes to the aims of the Horizon 2020 COST Action CA17116 SPRINT-*International Network for Translating Research on Perinatal Derivatives into Therapeutic Approaches* (S.B.).

References

[1] E. Braunwald, The war against heart failure: the Lancet lecture, Lancet 385 (2015) 812–824.
[2] M.A. Pfeffer, E. Braunwald, Ventricular remodeling after myocardial infarction. Experimental observations and clinical implications, Circulation 81 (1990) 1161–1172.
[3] M.G. Sutton, N. Sharpe, Left ventricular remodeling after myocardial infarction: pathophysiology and therapy, Circulation 101 (2000) 2981–2988.
[4] T.J. Cahill, R.P. Choudhury, P.R. Riley, Heart regeneration and repair after myocardial infarction: translational opportunities for novel therapeutics, Nat. Rev. Drug Discov. 16 (2017) 699–717.
[5] B. Zhou, Q. Ma, S. Rajagopal, S.M. Wu, I. Domian, J. Rivera-Feliciano, D. Jiang, A. von Gise, S. Ikeda, K.R. Chien, W.T. Pu, Epicardial progenitors contribute to the cardiomyocyte lineage in the developing heart, Nature. 454 (2008) 109–113.
[6] B. Zhou, L.B. Honor, H. He, Q. Ma, J.-H. Oh, C. Butterfield, R.-Z. Lin, J.M. Melero-Martin, E. Dolmatova, H.S. Duffy, A. von Gise, P. Zhou, Y.W. Hu, G. Wang, B. Zhang, L. Wang, J.L. Hall, M.A. Moses, F.X. McGowan, W.T. Pu, Adult mouse epicardium modulates myocardial injury by secreting paracrine factors, J. Clin. Invest. 121 (2011) 1894–1904.
[7] N. Smart, S. Bollini, K.N. Dubé, J.M. Vieira, B. Zhou, S. Davidson, D. Yellon, J. Riegler, A.N. Price, M.F. Lythgoe, W.T. Pu, P.R. Riley, De novo cardiomyocytes from within the activated adult heart after injury, Nature. 474 (2011) 640–644.
[8] O. Bergmann, R.D. Bhardwaj, S. Bernard, S. Zdunek, F. Barnabé-Heider, S. Walsh, J. Zupicich, K. Alkass, B.A. Buchholz, H. Druid, S. Jovinge, J. Frisén, Evidence for cardiomyocyte renewal in humans, Science. 324 (2009) 98–102.
[9] S.E. Senyo, M.L. Steinhauser, C.L. Pizzimenti, V.K. Yang, L. Cai, M. Wang, T.-D. Wu, J.-L. Guerquin-Kern, C.P. Lechene, R.T. Lee, Mammalian heart renewal by pre-existing cardiomyocytes, Nature 493 (2013) 433–436.
[10] E.R. Porrello, A.I. Mahmoud, E. Simpson, J.A. Hill, J.A. Richardson, E.N. Olson, H.A. Sadek, Transient regenerative potential of the neonatal mouse heart, Science. 331 (2011) 1078–1080.
[11] S.A. Jesty, M.A. Steffey, F.K. Lee, M. Breitbach, M. Hesse, S. Reining, J.C. Lee, R.M. Doran, A.Y. Nikitin, B.K. Fleischmann, M.I. Kotlikoff, c-kit+ precursors support postinfarction myogenesis in the neonatal, but not adult, heart, Proc. Natl. Acad. Sci. U. S. A. 109 (2012) 13380–13385.
[12] M. Gnecchi, P. Danieli, G. Malpasso, M.C. Ciuffreda, Paracrine mechanisms of mesenchymal stem cells in tissue repair, Methods Mol. Biol. 1416 (2016) 123–146.
[13] P. De Coppi, G. Bartsch, M.M. Siddiqui, T. Xu, C.C. Santos, L. Perin, G. Mostoslavsky, A.C. Serre, E.Y. Snyder, J.J. Yoo, M.E. Furth, S. Soker, A. Atala, Isolation of amniotic stem cell lines with potential for therapy, Nat. Biotechnol. 25 (2007) 100–106.

[14] A.A. Schiavo, C. Franzin, M. Albiero, M. Piccoli, G. Spiro, E. Bertin, L. Urbani, S. Visentin, E. Cosmi, G.P. Fadini, P. De Coppi, M. Pozzobon, Endothelial properties of third-trimester amniotic fluid stem cells cultured in hypoxia, Stem Cell Res Ther 6 (2015), 209.
[15] S. Bollini, K.K. Cheung, J. Riegler, X. Dong, N. Smart, M. Ghionzoli, S.P. Loukogeorgakis, P. Maghsoudlou, K.N. Dubé, P.R. Riley, M.F. Lythgoe, P. De Coppi, Amniotic fluid stem cells are cardioprotective following acute myocardial infarction, Stem Cells Dev. 20 (2011) 1985–1994.
[16] E. Lazzarini, C. Balbi, P. Altieri, U. Pfeffer, E. Gambini, M. Canepa, L. Varesio, M.C. Bosco, D. Coviello, G. Pompilio, C. Brunelli, R. Cancedda, P. Ameri, S. Bollini, The human amniotic fluid stem cell secretome effectively counteracts doxorubicin-induced cardiotoxicity, Sci. Rep. 6 (2016), 29994.
[17] C. Balbi, K. Lodder, A. Costa, S. Moimas, F. Moccia, T. van Herwaarden, V. Rosti, F. Campagnoli, A. Palmeri, P. De Biasio, F. Santini, M. Giacca, M.J. Goumans, L. Barile, A.M. Smits and S. Bollini, Supporting Data on In Vitro Cardioprotective and Proliferative Paracrine Effects by the Human Amniotic Fluid Stem Cell Secretome; Data in Brief - Submitted.
[18] C. Balbi, M. Piccoli, L. Barile, A. Papait, A. Armirotti, E. Principi, D. Reverberi, L. Pascucci, P. Becherini, L. Varesio, M. Mogni, D. Coviello, T. Bandiera, M. Pozzobon, R. Cancedda, S. Bollini, First characterization of human amniotic fluid stem cell extracellular vesicles as a powerful paracrine tool endowed with regenerative potential, Stem Cells Transl. Med. 6 (2017) 1340–1355.
[19] P. van Vliet, M. Roccio, A.M. Smits, A.A.M. van Oorschot, C.H.G. Metz, T.A.B. van Veen, J.P.G. Sluijter, P.A. Doevendans, M.-J. Goumans, Progenitor cells isolated from the human heart: a potential cell source for regenerative therapy, Neth. Hear. J. 16 (2008) 163–169.
[20] A.T. Moerkamp, K. Lodder, T. van Herwaarden, E. Dronkers, C.K.E. Dingenouts, F.C. Tengström, T.J. van Brakel, M.-J. Goumans, A.M. Smits, Human fetal and adult epicardial-derived cells: a novel model to study their activation, Stem Cell Res Ther 7 (2016), 174.
[21] B. Zhou, L.B. Honor, Q. Ma, J.-H. Oh, R.-Z. Lin, J.M. Melero-Martin, A. von Gise, P. Zhou, T. Hu, L. He, K.H. Wu, H. Zhang, Y. Zhang, W.T. Pu, Thymosin beta 4 treatment after myocardial infarction does not reprogram epicardial cells into cardiomyocytes, J. Mol. Cell. Cardiol. 52 (2012) 43–47.
[22] S. Dragoni, U. Laforenza, E. Bonetti, F. Lodola, C. Bottino, R. Berra-Romani, G. Carlo Bongio, M.P. Cinelli, G. Guerra, P. Pedrazzoli, V. Rosti, F. Tanzi, F. Moccia, Vascular endothelial growth factor stimulates endothelial colony forming cells proliferation and tubulogenesis by inducing oscillations in intracellular Ca2+ concentration, Stem Cells 29 (2011) 1898–1907.
[23] F. Lodola, U. Laforenza, F. Cattaneo, F.A. Ruffinatti, V. Poletto, M. Massa, R. Tancredi, E. Zuccolo, D.A. Khdar, A. Riccardi, M. Biggiogera, V. Rosti, G. Guerra, F. Moccia, VEGF-induced intracellular Ca2+ oscillations are down-regulated and do not stimulate angiogenesis in breast cancer-derived endothelial colony forming cells, Oncotarget 8 (2017) 95223–95246.
[24] J. Tóvári, R. Gilly, E. Rásó, S. Paku, B. Bereczky, N. Varga, Á. Vágó, J. Tímár, Recombinant human erythropoietin α targets intratumoral blood vessels, improving chemotherapy in human xenograft models, Cancer Res. 65 (2005) 7186–7193.
[25] A. Eulalio, M. Mano, M. Dal Ferro, L. Zentilin, G. Sinagra, S. Zacchigna, M. Giacca, M.D. Ferro, L. Zentilin, G. Sinagra, S. Zacchigna, M. Giacca, Functional screening identifies miRNAs inducing cardiac regeneration, Nature 492 (2012) 376–381.
[26] M. Arif, R. Pandey, P. Alam, S. Jiang, S. Sadayappan, A. Paul, R.P.H. Ahmed, MicroRNA-210-mediated proliferation, survival, and angiogenesis promote cardiac repair post myocardial infarction in rodents, J. Mol. Med. 95 (2017) 1369–1385.
[27] A.G.-E.E. Ibrahim, K. Cheng, E. Marbán, Exosomes as critical agents of cardiac regeneration triggered by cell therapy, Stem Cell Rep. 2 (2014) 606–619.
[28] K.S. Rao, A. Aronshtam, K.L. McElory-Yaggy, B. Bakondi, P. VanBuren, B.E. Sobel, J.L. Spees, Human epicardial cell-conditioned medium contains HGF/IgG complexes that phosphorylate RYK and protect against vascular injury, Cardiovasc. Res. 107 (2015) 277–286.
[29] T. Kempf, M. Eden, J. Strelau, M. Naguib, C. Willenbockel, J. Tongers, J. Heineke, D. Kotlarz, J. Xu, J.D. Molkentin, H.W. Niessen, H. Drexler, K.C. Wollert, The transforming growth factor-beta superfamily member growth-differentiation factor-15 protects the heart from ischemia/reperfusion injury, Circ. Res. 98 (2006) 351–360.
[30] Y. Zhang, X. Liang, S. Liao, W. Wang, J. Wang, X. Li, Y. Ding, Y. Liang, F. Gao, M. Yang, Q. Fu, A. Xu, Y.-H. Chai, J. He, H.-F. Tse, Q. Lian, Potent paracrine effects of human induced pluripotent stem cell- derived mesenchymal stem cells attenuate doxorubicin-induced cardiomyopathy, Nat. Publ. Group 5 (2015), 11235.
[31] N.A. Trueblood, Z. Xie, C. Communal, F. Sam, S. Ngoy, L. Liaw, A.W. Jenkins, J. Wang, D.B. Sawyer, O.H. Bing, C.S. Apstein, W.S. Colucci, K. Singh, Exaggerated left ventricular dilation and reduced collagen deposition after myocardial infarction in mice lacking osteopontin, Circ. Res. 88 (2001) 1080–1087.
[32] X. Xu, J. Pang, Y. Chen, R. Bucala, Y. Zhang, J. Ren, Macrophage migration inhibitory factor (MIF) deficiency exacerbates aging-induced cardiac remodeling and dysfunction despite improved inflammation: role of autophagy regulation, Sci. Rep. 6 (2016), 22488.
[33] A. Miyawaki, M. Obana, Y. Mitsuhara, A. Orimoto, Y. Nakayasu, T. Yamashita, S.-I. Fukada, M. Maeda, H. Nakayama, Y. Fujio, Adult murine cardiomyocytes exhibit regenerative activity with cell cycle reentry through STAT3 in the healing process of myocarditis, Sci. Rep. 7 (2017), 1407.
[34] C. Han, Y. Nie, H. Lian, R. Liu, F. He, H. Huang, S. Hu, Acute inflammation stimulates a regenerative response in the neonatal mouse heart, Cell Res. 25 (2015) 1137–1151.
[35] T. Mirabella, M. Cilli, S. Carlone, R. Cancedda, C. Gentili, Amniotic liquid derived stem cells as reservoir of secreted angiogenic factors capable of stimulating neoarteriogenesis in an ischemic model, Biomaterials. 32 (2011) 3689–3699.
[36] T. Mirabella, J. Hartinger, C. Lorandi, C. Gentili, M. van Griensven, R. Cancedda, Proangiogenic soluble factors from amniotic fluid stem cells mediate the recruitment of endothelial progenitors in a model of ischemic fasciocutaneous flap, Stem Cells Dev. 21 (2012) 2179–2188.
[37] S. Dragoni, M. Reforgiato, E. Zuccolo, V. Poletto, F. Lodola, F.A. Ruffinatti, E. Bonetti, G. Guerra, G. Barosi, V. Rosti, F. Moccia, Dysregulation of VEGF-induced proangiogenic Ca2+ oscillations in primary myelofibrosis-derived endothelial colony-forming cells, Exp. Hematol. 43 (2015) 1019–1030.e3.
[38] F. Moccia, F. Tanzi, L. Munaron, Endothelial remodelling and intracellular calcium machinery, Curr. Mol. Med. 14 (2014) 457–480.
[39] F. Moccia, G. Bertoni, A.F. Pla, S. Dragoni, E. Pupo, A. Merlino, D. Mancardi, L. Munaron, F. Tanzi, Hydrogen sulfide regulates intracellular Ca2+ concentration in endothelial cells from excised rat aorta, Curr. Pharm. Biotechnol. 12 (2011) 1416–1426.
[40] T. Eschenhagen, R. Bolli, T. Braun, L.J. Field, B.K. Fleischmann, J. Frisén, M. Giacca, J.M. Hare, S. Houser, R.T. Lee, E. Marbán, J.F. Martin, J.D. Molkentin, C.E. Murry, P.R. Riley, P. Ruiz-Lozano, H.A. Sadek, M.A. Sussman, J.A. Hill, Cardiomyocyte regeneration: a consensus statement, Circulation. 136 (2017) 680–686.
[41] F. Beretti, M. Zavatti, F. Casciaro, G. Comitini, F. Franchi, V. Barbieri, G.B. La Sala, T. Maraldi, Amniotic fluid stem cell exosomes: therapeutic perspective, Biofactors. 44 (2018) 158–167.
[42] G.N. Huang, J.E. Thatcher, J. McAnally, Y. Kong, X. Qi, W. Tan, J.M. DiMaio, J.F. Amatruda, R.D. Gerard, J.A. Hill, R. Bassel-Duby, E.N. Olson, C/EBP transcription factors mediate epicardial activation during heart development and injury, Science. 338 (2012) 1599–1603.
[43] A. Lepilina, A.N. Coon, K. Kikuchi, J.E. Holdway, R.W. Roberts, C.G. Burns, K.D. Poss, A dynamic epicardial injury response supports progenitor cell activity during zebrafish heart regeneration, Cell. 127 (2006) 607–619.
[44] F. Limana, C. Bertolami, A. Mangoni, A. Di Carlo, D. Avitabile, D. Mocini, P. Iannelli, R. De Mori, C. Marchetti, O. Pozzoli, C. Gentili, A. Zacheo, A. Germani, M.C. Capogrossi, Myocardial infarction induces embryonic reprogramming of epicardial c-kit+ cells: role of the pericardial fluid, J. Mol. Cell. Cardiol. 48 (2010) 609–618.
[45] K.N. Dubé, T.M. Thomas, S. Munshaw, M. Rohling, P.R. Riley, N. Smart, Recapitulation of developmental mechanisms to revascularize the ischemic heart, JCI Insight 2 (2017)https://doi.org/10.1172/jci.insight.96800.
[46] K.R. Vrijsen, J.A. Maring, S.A.J. Chamuleau, V. Verhage, E.A. Mol, J.C. Deddens, C.H.G. Metz, K. Lodder, E.C.M. van Eeuwijk, S.M. van Dommelen, P.A. Doevendans, A.M. Smits, M.-J. Goumans, J.P.G. Sluijter, Exosomes from cardiomyocyte progenitor cells and mesenchymal stem cells stimulate angiogenesis via EMMPRIN, Adv. Healthc. Mater. 5 (2016) 2555–2565.
[47] S.K. Das, S.K. Bhutia, B. Azab, T.P. Kegelman, L. Peachy, P.K. Santhekadur, S. Dasgupta, R. Dash, P. Dent, S. Grant, L. Emdad, M. Pellecchia, D. Sarkar, P.B. Fisher, MDA-9/syntenin and IGFBP-2 promote angiogenesis in human melanoma, Cancer Res. 73 (2013) 844–854.
[48] A.A. Hellingman, J.J. Zwaginga, R.T. van Beem, J.F. TeRM/Smart Mix Consortium, J.F. Hamming, W.E. Fibbe, P.H.A. Quax, S.B. Geutskens, T-cell-pre-stimulated monocytes promote neovascularisation in a murine hind limb ischaemia model, Eur. J. Vasc. Endovasc. Surg. 41 (2011) 418–428.
[49] M. Suarez-Carmona, M. Bourcy, J. Lesage, N. Leroi, L. Syne, S. Blacher, P. Hubert, C. Erpicum, J.-M. Foidart, P. Delvenne, P. Birembaut, A. Noël, M. Polette, C. Gilles, Soluble factors regulated by epithelial-mesenchymal transition mediate tumour angiogenesis and myeloid cell recruitment, J. Pathol. 236 (2015) 491–504.